haematologica
Journal of the Ferrata Storti Foundation

FOXM1 down-regulation is a trigger of isatuximab-induced direct cell death in multiple myeloma cells with 1q+

by Jiro Kikuchi, Naoki Osada, Sae Matsuoka, Tomomi Ohta, Hirotaka Kazama, Heigoro Shirai, Marco Meloni, Marielle Chiron, Hiroshi Yasui, Hideki Nakasone and Yusuke Furukawa

Received: March 25, 2025.
Accepted: July 21, 2025.

Citation: Jiro Kikuchi, Naoki Osada, Sae Matsuoka, Tomomi Ohta, Hirotaka Kazama, Heigoro Shirai, Marco Meloni, Marielle Chiron, Hiroshi Yasui, Hideki Nakasone and Yusuke Furukawa. FOXM1 down-regulation is a trigger of isatuximab-induced direct cell death in multiple myeloma cells with 1q+. Haematologica. 2025 July 31. doi: 10.3324/haematol.2025.287904 [Epub ahead of print]

FOXM1 down-regulation is a trigger of isatuximab-induced direct cell death in multiple myeloma cells with 1q+

Jiro Kikuchi[1], Naoki Osada[1], Sae Matsuoka[1], Tomomi Ohta[2], Hirotaka Kazama[2], Heigoro Shirai[2], Marco Meloni[3], Marielle Chiron[3], Hiroshi Yasui[4,5], Hideki Nakasone[1], and Yusuke Furukawa[1,6].

[1]Division of Emerging Medicine for Integrated Therapeutics (EMIT), Center for Molecular Medicine, Jichi Medical University, Shimotsuke, Tochigi 329-0498, Japan; [2]SANOFI Oncology Medical, Tokyo 163-1488, Japan; [3]SANOFI R&D, Vitry-sur-Seine, France; [4]Department of Hematology/Oncology, The Institute of Medical Science, University of Tokyo, Tokyo 108-8639, Japan; [5]Department of Hematology & Oncology, St. Marianna University School of Medicine, Kawasaki 216-8511 Japan; [6]Center for Medical Education, Teikyo University of Science, Tokyo 120-0045, Japan.

Running title: Isatuximab down-regulates FOXM1 in 1q+ MM cells.

Correspondence: Jiro Kikuchi Ph.D., Division of Emerging Medicine for Integrated Therapeutics (EMIT), Center for Molecular Medicine, Jichi Medical University, 3311-1 Yakushiji, Shimotsuke, Tochigi 329-0498, Japan.
E-mail: kiku-j@jichi.ac.jp; Tel.: +81-285-58-7400; Fax: +81-285-44-7501

Authors' contributions: J.K. performed experiments, analyzed data, and drafted and finalized the manuscript; N.S. and S.M. performed experiments and analyzed data; T.O., H.K., H.S., M.M, M.C., H.Y., and H.N. provided materials and critically reviewed the manuscript; and Y.F. supervised research. All authors read and approved the manuscript before submission.

Data-sharing Statement: For original data, please contact kiku-j@jichi.ac.jp. ChIP-sequence data are available at GEO under accession number GSE279782.

Conflict of Interest

This study was funded by Sanofi. T.O., H.K., H.S., M.M, and M.C, are employees of Sanofi.

Acknowledgements

We are grateful to Ms. Mayuka Shiino, Ms. Mai Tadaki, and Ms. Akiko Yonekura for their excellent technical assistance.

Funding

This work was supported by a Sanofi Research Grant (to J.K., and Y.F.), Grant-in-Aid for Scientific Research from JSPS, and the Japan Leukemia Research Fund (to J.K., N.O., and Y.F.), and J.K. was funded by Takeda Science Foundation, Chugai Foundation for Innovative Drug Discovery Science, Princess Takamatsu Cancer Research Fund, and the International Myeloma Foundation Japan's Grant.

To the Editor:

Targeted therapies like proteasome inhibitors (PIs), immunomodulatory drugs (IMiDs), and/or anti-CD38 antibody have significantly improved the prognosis of patients with multiple myeloma (MM) [1,2]. However, the prognoses with high-risk chromosome abnormalities (CAs), such as t(4;14), t(14;16), del(17p), and gain/amplification of 1q (designated as 1q+), remain poor [3]. The anti-CD38 antibody, isatuximab, can significantly prolong the progression-free survival of relapsed and refractory MM (RRMM) patients carrying 1q+ [4]. However, daratumumab, another anti-CD38 antibody, has been largely ineffective [5]. While both antibodies confer antibody-dependent immune effector cell-mediated cytotoxicity, isatuximab can directly induce the death of MM cells even in the absent of immune effector cells [6]. This led us to hypothesize that direct cell death may provide clinical benefit to MM patients with 1q+.

A previous study has shown that the transcription factor PBX1, which is in the 1q23 region, is strongly associated with poor prognosis of MM patients with 1q+. PBX1 is overexpressed in 1q+ MM cells and confers drug resistance by transactivating the downstream target genes including E2F1/E2F2, FOXM1, and NEK2 [7]. Of these, we found significant upregulation of these factors in 1q+ MM cells, and that high expression levels of FOXM1, E2F2, or MCL1 were associated with worse prognosis in 1q+ MM patients after total therapy 2 and 3 (TT2/3) (Supplementary Fig.S1A). In addition, FOXM1 was essentially found to be expressed only in the 1q+ MM cell lines compared to the cells with a normal copy number of 1q (designated as $1q^{normal}$ throughout the manuscript). In contrast, E2F2 showed a variable expression pattern among the 1q+ MM cell lines, while MCL1 was expressed in all cell lines regardless of 1q copy number (Fig.1A, and Supplementary Fig.S1B). Furthermore, both genetic knockdown and pharmacological inhibition of FOXM1 significantly inhibited the growth of 1q+ MM cell lines but did not have any impact on

the $1q^{normal}$ cell lines (Supplementary Fig.S1C). These results suggest an indispensable role of FOXM1 in the growth and survival of 1q+ MM cells.

There is evidence that isatuximab can directly induce death of CD38-overexpressing MM cells.[13,14] To this end, we overexpressed the *CD38* gene in the KMM.1 and KMS28-BM sublines that respectively harbor 6 copies of 1q (1q amp) and 3 copies of 1q (1q gain) with t(4;14). As expected, isatuximab significantly inhibited the growth of both sublines even in cells with high risk CAs, along with marked incorporation of isatuximab into MM cells. However, other antibodies, Elo-m and Dara-m, did not have any impact on the sublines (Fig.1B). We also determined the effect of these antibodies on the expression of FOXM1, E2F2, and MCL1 in the two sublines. Of these, we found that isatuximab downregulated FOXM1 protein expression in both sublines (Fig.1B and Supplementary Fig.S1D). Consistent with these results, isatuximab downregulated FOXM1 in primary MM cells derived from patients with 1q+, but not in the $1q^{normal}$ cells (Supplementary Fig.1E). Informed consent was obtained in accordance with the Declaration of Helsinki, and the protocol was approved by the Institutional Review Board of Jichi Medical University. On the other hand, no significant changes were detected in the expression of E2F2 and MCL1 in either subline (Fig.1B and Supplementary Fig.S1D). In addition, Elo-m and Dara-m had no significant effect in their expression levels (Fig.1B). A previous study had shown that the uptake of large amount of monoclonal antibodies into the cells led to the enlargement and degradation of lysosomes, and the subsequent degradation of intracellular proteins by lysosomal proteases like cathepsins triggered non-apoptotic lysosomal cell death (LCD). In addition, concanamycin A (Con-A), an inhibitor of vacuolar ATPases, suppressed LCD by blocking antibody-induced lysosomal enlargement and degradation [8]. Consistent with the results, we found that Con-A mitigated isatuximab-induced growth inhibition, which coincided with restored

FOXM1 expression (Fig.1C). These results suggest that FOXM1 protein is likely degraded by the lysosomal proteases. In contrast, daratumumab was not sufficiently incorporated into the MM cells to induce FOXM1 protein degradation by lysosomal proteases (Fig.1B).

To further validate the mechanism underlying isatuximab-induced growth inhibition, we established two FOXM1-overexpressing MM cell lines. As expected, forced expression of FOXM1 significantly mitigated the inhibitory effects of isatuximab in both sublines. In contrast, FOXM1 knockdown augmented isatuximab-induced growth inhibition (Supplementary Fig.S1F). Given that reactive oxygen species (ROS) mediate antibody-induced direct cell death [9], and FOXM1 inhibitor can trigger ROS production in cancer cells [10,11], we also measured the intracellular ROS levels. Consistent with the results, the FOXM1 inhibitor thiostrepton significantly inhibited the growth of MM cells by enhancing ROS production (Supplementary Fig.S1G). In addition, forced expression of FOXM1 significantly suppressed ROS production (Fig.1D). These results suggest that isatuximab downregulates the FOXM1 protein by lysosomal protease-mediated degradation, resulting in direct cell death through ROS production in 1q+ MM cells.

Recent clinical trials have shown that isatuximab in combination with pomalidomide (Poma) or carfilzomib (CFZ) prolonged the survival of RRMM patients with 1q+ [4]. Previous studies revealed that both Poma and CFZ can induce caspase-dependent apoptosis and trigger ROS production in MM cells [12,13]. In addition, several anti-cancer drugs exert their cytotoxic effects via caspase-dependent degradation of transcriptional regulators like Sp1 or histone deacetylases (HDACs) [14,15]. In line with these studies, we found that Poma and CFZ additively enhanced isatuximab-induced cell death and increased ROS production by promoting downregulation of FOXM1 protein (Fig.2A and Supplementary Fig.S1H). Since treatment with Poma and CFZ, and

not isatuximab, activated caspase-3, caspase-8, and PARP (Fig.2A), we surmise that FOXM1 downregulation may be caused by caspase-dependent degradation. On the other hand, isatuximab-induced cell death is independent of caspases. Taken together, Poma and CFZ additively enhanced isatuximab-induced cell death by enhancing FOXM1 downregulation and ROS production.

To identify the downstream targets of FOXM1 in situ, we analyzed its binding sites in the genome of KMM.1 cells using chromatin immunoprecipitation with high-throughput DNA sequencing (ChIP-seq). As shown in Supplemenatry Fig.S2A, over 70% of the peaks corresponding to FOXM1 binding sites located in the vicinity of transcription start sites (TSSs). FOXM1 bound to the TSSs of genes closely related to MM progression including several genes, such as *NEK2*, *RGS5*, *UBE2T*, *ANP32E*, and *FAM72A* localized at 1q region. In addition, we found co-occupancy with the H3K27-acetylated regions in the regulatory regions in the 1q+ MM cells but not in the $1q^{normal}$ cells (Fig.2B and Supplementary Fig.S2B). Although all target genes were upregulated in the 1q+ MM cells, the expression levels of *NEK2*, *UBE2T*, and *FAM72A* showed a significant positive correlation to that of *FOXM1* and the overexpression was significantly associated with worse survival of 1q+ MM patients following TT2/3 (Supplementary Fig.S2C). Likewise, both NEK2 and UBE2T were significantly upregulated in the 1q+ MM cell lines compared to the $1q^{normal}$ cells (Fig.2C). Next, we found that both genetic knockdown and pharmacological inhibition of FOXM1 significantly downregulated NEK2 and UBE2T proteins and mRNAs (Supplementary Fig.S3A and S3B). Furthermore, forced expression of NEK2 and UBE2T significantly mitigated the thiostrepton-induced growth inhibition (Supplementary Fig.S3C and S3D). These results suggest that NEK2 and UBE2T are the critical downstream targets of FOXM1 in 1q+ MM cells.

We next screened for the global isatuximab-mediated transcriptomic changes in KMM.1-38 cells and found that isatuximab reduced the expression of several genes including NEK2 and UBE2T (Fig.3A). As anticipated, isatuximab significantly downregulated NEK2 and UBE2T proteins and mRNAs in a dose-dependent manner, which correlated with the cytotoxic effects (Fig.3B). In addition, isatuximab also downregulated NEK2 and UBE2T in primary MM cells derived from patients with 1q+ (Supplementary Fig.S3E). Consistent with the above findings, overexpression of NEK2 and UBE2T partially mitigated the inhibitory effects of isatuximab (Fig.3C). These results suggest that isatuximab induces direct death in 1q+ MM cells via downregulation of the FOXM1/NEK2/UBE2T axis.

In conclusion, we have shown that isatuximab exerts direct cell death to 1q+ MM cells by downregulating the FOXM1 protein, followed by ROS production and the inactivation of *NEK2* and *UBE2T* genes. Poma and CFZ additively enhanced the cytotoxicity in combination with isatuximab by promoting FOXM1 downregulation and ROS production. However, this study has several limitations. First, we could not obtain sufficient number of cells from MM patients to reproduce all data using primary MM cells. Second, we could not confirm that Dara-m and Elo-m are identical to the commercial Dara and Elo. Nevertheless, our findings suggest that isatuximab exerts direct cell death to 1q+ MM cells by targeting the FOXM1/NEK2/UBE2T axis and provide a rationale for isatuximab-based therapy for the treatment of 1q+ MM patients from basic standpoints for the first time.

References

1. Attal M, Lauwers-Cances V, Hulin C, et al. Lenalidomide, bortezomib, and dexamethasone with transplantation for myeloma. N Engl J Med. 2017;376(14):1311-1320.
2. Facon T, Kumar S, Plesner T, et al. Daratumumab plus lenalidomide and dexamethasone for untreated myeloma. N Engl J Med. 2019;380(22):2104-2115.
3. Pawlyn C, Cairns D, Kaiser M, et al. The relative importance of factors predicting outcome for myeloma patients at different ages: results from 3894 patients in the Myeloma XI trial. Leukemia. 2020;34(2):604-612.
4. Martin T, Richardson PG, Facon T, et al. Primary outcomes by 1q21+ status for isatuximab-treated patients with relapsed/refractory multiple myeloma: subgroup analyses from ICARIA-MM and IKEMA. Haematologica. 2022;107(10):2485-2491.
5. Mohan M, Weinhold N, Schinke C, et al. Daratumumab in high-risk relapsed/refractory multiple myeloma patients: adverse effect of chromosome 1q21 gain/amplification and GEP70 status on outcome. Br J Haematol. 2020;189(1):67-71.
6. Zhu C, Song Z, Wang A, et al. Isatuximab acts through Fc-dependent, independent, and direct pathways to kill multiple myeloma cells. Front Immunol. 2020;11:1771.
7. Trasanidis N, Katsarou A, Ponnusamy K, et al. Systems medicine dissection of chr1q-amp reveals a novel PBX1-FOXM1 axis for targeted therapy in multiple myeloma. Blood. 2022;139(13):1939-1953.
8. Ivanov A, Beers SA, Walshe CA, et al. Monoclonal antibodies directed to CD20 and HLA-DR can elicit homotypic adhesion followed by lysosome-mediated cell death in human lymphoma and leukemia cells. J Clin Invest. 2009;119(8):2143-5219.

9. Honeychurch J, Alduaij W, Azizyan M, et al. Antibody-induced nonapoptotic cell death in human lymphoma and leukemia cells is mediated through a novel reactive oxygen species-dependent pathway. Blood. 2012;119(15):3523-3533.
10. Su G, Yang Q, Zhou H, et al. Thiostrepton as a potential therapeutic agent for hepatocellular carcinoma. Int J Mol Sci. 2024;25(17):9717.
11. Okuni N, Honma Y, Urano T, Tamura K. Romidepsin and tamoxifen cooperatively induce senescence of pancreatic cancer cells through downregulation of FOXM1 expression and induction of reactive oxygen species/lipid peroxidation. Mol Biol Rep. 2022;49(5):3519-3529.
12. Sebastian S, Zhu YX, Braggio E, et al. Multiple myeloma cells' capacity to decompose H_2O_2 determines lenalidomide sensitivity. Blood. 2017;129(8):991-1007.
13. Fink EE, Mannava S, Bagati A, et al. Mitochondrial thioredoxin reductase regulates major cytotoxicity pathways of proteasome inhibitors in multiple myeloma cells. Leukemia. 2016;30(1):104-111.
14. Kikuchi J, Wada T, Shimizu R, et al. Histone deacetylases are critical targets of bortezomib-induced cytotoxicity in multiple myeloma. Blood. 2010;116(3):406-417.
15. Hiraoka N, Kikuchi J, Koyama D, et al. Alkylating agents induce histone H3K18 hyperacetylation and potentiate HDAC inhibitor-mediated global histone acetylation and cytotoxicity in mantle cell lymphoma. Blood Cancer J. 2013;3(12):e169.

Figure Legends

Fig.1. Isatuximab downregulates FOXM1 protein and induces ROS-mediated direct cell death in 1q+ MM cells.

[A] Whole cell lysates were prepared from 1q+ and $1q^{normal}$ MM cell lines and subjected to immunoblot for FOXM1, E2F2, and MCL1 using GAPDH as the loading control. Immunoblotting was carried out according to a standard method using the following antibodies: anti-FOXM1 (#20459), anti-MCL1 (#4572) (Cell Signaling Technology [CST], MA, USA); anti-E2F2 (sc-9967), and anti-GAPDH (Santa Cruz Biotechnology, CA, USA). The copy number of chromosome 1q was detected by fluorescence in situ hybridization (FISH) using the CKS1B FISH probe; 1q gain was defined as having 3 copies of CKS1B, and 1q amp was defined as having ≥4 copies of CKS1B. MM cell lines KMS12BM, JJN3, and SKMM1 with 2 copies of chromosome 1q (normal), KMS26, KMS28-BM, KMS-28PE (K28PE), KMS34, KMS11, RPMI8226, MM1.S, KMS21, NCI-H929, and MOLP8 with 3 copies of chromosome 1q (1q gain), and KMM.1, KHM1B (KHM), Delta47 (Del47), and KMS20 with 4< copies of chromosome 1q (1q amp) were procured from Health Science Research Resources Bank. In addition, KMS12BM, SKMM1, and MOLP8 harbor t(11;14). KMS26, KMS28-BM, KMS28-PE, KMS34, KMS11, and NCI-H929 harbor t(4;14). The FISH analyses were outsourced to SRL Inc. (Tokyo, Japan). [B] CD38-overexpressing KMM.1 and KMS28-BM sublines were established (denoted as KMM.1-38 and KMS28BM-38 respectively), and cultured in the presence of 5 μg/mL human immunoglobulin (hIgG), elotuzumab-mimic (Elo-m), daratumumab-mimic (Dara-m), and isatuximab (Isa) for 24 h. We used the lentiviral vector CSII-CMV-MCS-IRES-VENUS (provided by Dr. Hiroyuki Miyoshi, RIKEN BioResource Center, Ibaraki, Japan) containing the coding regions of *CD38* cDNA. Upper panel: Cytospin specimens were prepared and stained with FITC conjugated anti-hIgG antibody (green). Nuclei

were counterstained with DAPI (blue). Only merged images are shown. Middle panel: Cell proliferation was assessed by the MTT reduction assay using the Cell Counting Kit (Wako Biochemicals, Osaka, Japan). Data is shown relative to that of the corresponding hIgG controls. Data are the means ± S.D. (bars) of multiple independent experiments (n = 3); *P <0.05 compared to the corresponding hIgG control was determined by one-way ANOVA with Student-Newman-Keuls multiple comparison test. The KaleidaGraph software (Synergy Software, Reading, PA, USA) was used for all statistical analyses. P values less than 0.05 were considered significant. Lower panel: Immunoblot showing the expression of FOXM1, E2F2, MCL1, and GAPDH (loading control). [C] KMM.1-38 and KMS28BM-38 cells were cultured in the presence of Isa at the indicated concentrations with or without 1nM concanamycin A (Con-A) for 24 h. Upper panel: Cell proliferation was assessed by the MTT reduction assay and the data is shown relative to that of the corresponding untreated controls. Data are the means ± S.D. (bars) of multiple independent experiments (n = 3); P values were determined by one-way ANOVA with a Student-Newman-Keuls multiple comparison test. Lower panel: Immunoblot showing the expression of FOXM1 and GAPDH (loading control). [D] KMM.1-38 and KMS28BM-38 cells were transduced with FOXM1-expressing (FOX) or empty (mock) lentiviral vector, and the stable transformants were cultured with different concentrations of isatuximab (Isa) for 24 h. We used the lentiviral vector CSII-CMV-MCS-IRES-VENUS containing the coding regions of *FOXM1* cDNA for gain-of-function experiments. Left panel: Cell proliferation was assessed by the MTT reduction assay and the data is shown relative to that of the corresponding untreated controls. Data are the means of multiple independent experiments (n > 3). S.D. was less than 10% and thus omitted; *P < 0.05 by one-way ANOVA with Student-Newman-Keuls multiple comparison test. Right panel: The transformants were cultured with or without 5 μg/mL isatuximab for 24 h. Upper right panel:

Immunoblot showing the expression of FOXM1 and GAPDH (loading control) in the indicated groups. Lower right panel: ROS levels were assessed using the ROS assay kit (DOJINDO, Tokyo, Japan) and the data is shown relative to that of the untreated controls. Data are the means ± S.D. (bars) of multiple independent experiments (n = 3); *P* values were determined by one-way ANOVA with Student-Newman-Keuls multiple comparison test.

Fig.2. Combined effects of isatuximab with pomalidomide or carfilzomib and global analysis of FOXM1 binding in the genome of 1q+ MM cells.

[A] KMM.1-38 and KMS28BM-38 cells were treated with vehicle (None), 2.5 μg/ml Isa, 2 μM pomalidomide (Poma), 2 nM carfilzomib (CFZ), or their combinations (Isa+Poma or Isa+CFZ) for 24 h. Upper panel: Cell proliferation was assessed by the MTT reduction assay and the data is shown relative to that of the corresponding untreated controls (None). Data are the means ± S.D. (bars) of multiple independent experiments (n = 3); *P* values were determined by one-way ANOVA with Student-Newman-Keuls multiple comparison test. Middle panel: Immunoblot showing the expression of FOXM1, cleaved caspase-3 (c-casp.3), cleaved caspase-8 (c-casp.8), and cleaved PARP (c-PARP) and GAPDH (loading control) in the indicated groups. Immunoblotting was carried out according to a standard method using the following antibodies: anti-cleaved caspase-3 (#9661), anti-cleaved caspase-8 (#9496), and anti-cleaved PARP (#9541) (Cell Signaling Technology). Lower panel: ROS levels were assessed using the ROS assay kit and the data is shown relative to that of the corresponding untreated controls (None). Data are the means ± S.D. (bars) of multiple independent experiments (n = 3); *P* values were determined by one-way ANOVA with Student-Newman-Keuls multiple comparison test. [B] KMM.1 cells were fixed in 1% formaldehyde at room temperature for 10 min and chromatin fractions were isolated by enzymatic shearing. Chromatin immunoprecipitation sequencing (ChIP-seq) was outsourced to

Active Motif (Carlsbad, CA, USA), and the data and protocols have been deposited in a MINSEQE-compliant GEO database under accession number GSE279782. We used an antibody against FOXM1 (#20459, CST) validated by Active Motif. Left panel: The peak values of FOXM1 binding sites in the selected genes in KMM.1 cells. Right panel: Heat map of the FOXM1/H3K27ac binding at the promoter/enhancer regions of representative genes based on ChIP-seq data. The ChIP-seq data of the following cell types was used: MM.1S (SRX20095564), KMS28BM (SRX7798959), KMS12BM (SRX7798957), and normal plasma cells isolated from healthy volunteers (NPCs) (SRX7798977). [C] Immunoblot showing the expression of NEK2, UBE2T, ANP32E, and GAPDH (loading control) in the 1q+ and $1q^{normal}$ MM cell lines. Immunoblotting was carried out according to a standard method using the following antibodies: anti-NEK2 (#14233), anti-UBE2T (#10105) (Proteintech Inc, IL, USA), and anti-ANP32E (#AP20559) (Abcepta, CA, USA).

Fig.3. Isatuximab downregulates the expression of NEK2 and UBE2T, both of which were critical downstream targets of FOXM1.

[A] KMM.1-38 cells were cultured with 5 μg/mL isatuximab (KMM.1-38+Isa) or isotype matched hIgG (KMM.1-38+IgG) for 24 h, and the RNA fractions were isolated. Microarray analysis was performed for 32,078 genes including microRNAs. Red lines correspond to 2-fold changes ($P < 0.05$ with a false discovery rate [FDR] threshold of 0.05). Several genes located in chromosome 1q region are annotated. [B] KMM.1-38 and KMS28BM-38 cells were treated with different concentrations of isatuximab for 24 h. Upper panel: Cell proliferation was assessed by the MTT reduction assay and the data is shown relative to that of the corresponding untreated controls. Data are the means ± S.D. (bars) of multiple independent experiments (n = 3). $*P < 0.05$ by one-way ANOVA with Student-Newman-Keuls multiple comparison test. Middle panel: Total cellular RNA

was isolated from 1-10 x 10^4 cells using an RNeasy Kit (Qiagen, CA, USA), reverse-transcribed into complementary DNA using ReverTra Ace and oligo(dT) primers (Toyobo, Tokyo, Japan), and subjected to real-time quantitative RT-PCR (QPCR) using the specific primers. The expression levels of candidate FOXM1-target genes (*NEK2*, *UBE2T*, and *ANP32E*) were quantified by the $2^{-\Delta\Delta Ct}$ method using *GAPDH* as the reference and shown as fold changes against untreated control set at 1.0. The means ± S.D. (bars) are of multiple independent experiments (n = 3). *$P < 0.05$ by one-way ANOVA with a Student-Newman-Keuls multiple comparison test. We used TaqMan Fast Universal PCR Master Mix and Expression Assays (Hs06629033 for *NEK2*, Hs00928040 for *UBE2T*, Hs05029891 for *ANP32E*, and Hs01922876 for *GAPDH* (Thermo Fisher Scientific, MA, USA). Lower panel: Immunoblot showing expression of FOXM1, NEK2, UBE2T, ANP32E, and GAPDH proteins (loading control) in the indicated groups. [C] KMM.1-38 and KMS28BM-38 cells were transduced with either an empty lentiviral vector (mock), NEK2-overexpressing vector (NEK2), or UBE2T-overexpressing vector (UBE) and the stable transformants were treated with different concentrations of isatuximab for 24 h. We used the lentiviral vector CSII-CMV-MCS-IRES-VENUS containing the coding regions of *NEK2* and *UBE2T* cDNA for gain-of-function experiments. Cell proliferation was assessed by the MTT reduction assay and the data is shown relative to that of the corresponding untreated controls. Data are the means of multiple experiments (n > 3); S.D. was less than 10% and thus omitted. *$P < 0.05$ by one-way ANOVA with Student-Newman-Keuls multiple comparison test.

Fig. 1

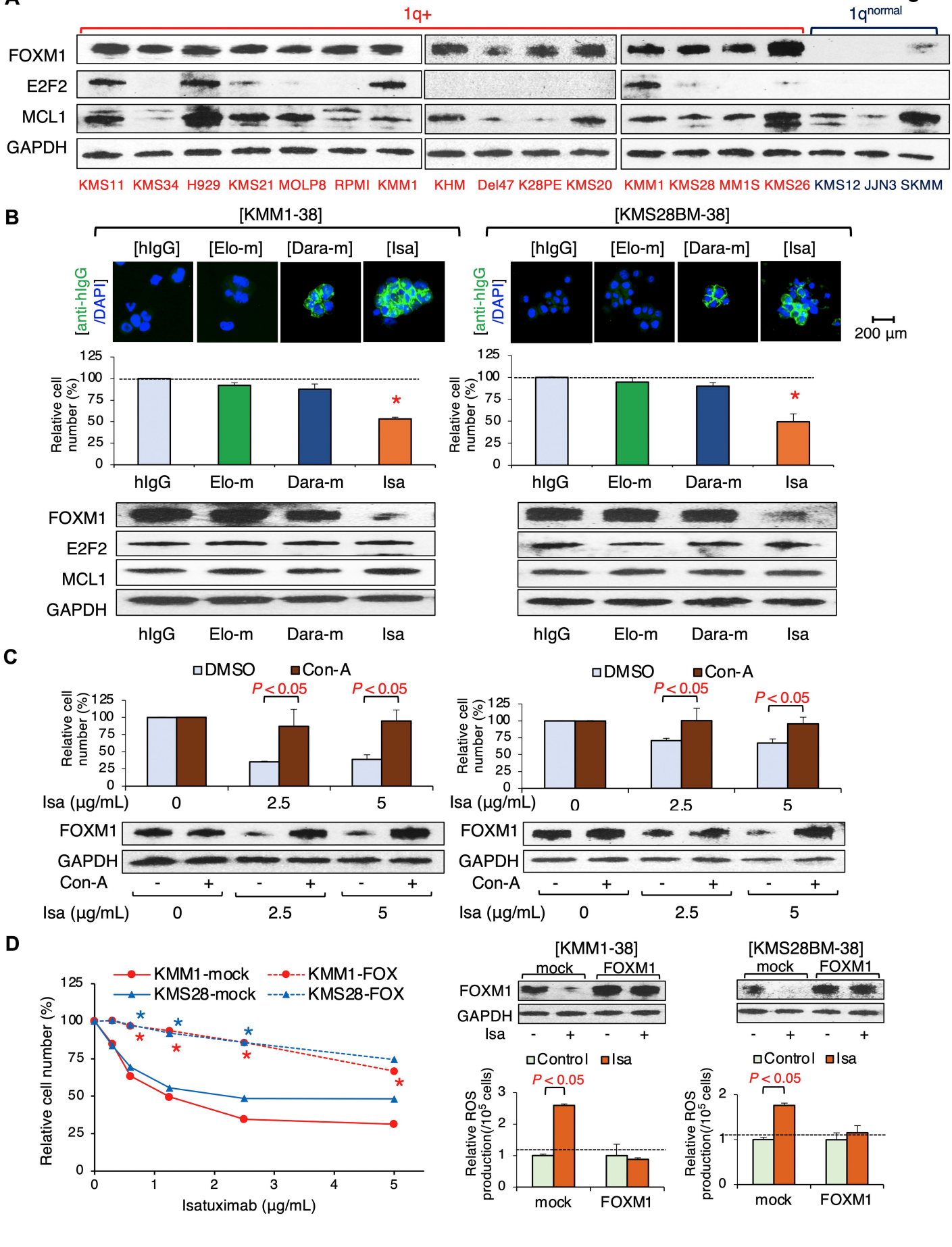
A
1q+
1q^normal
FOXM1
E2F2
MCL1
GAPDH
KMS11 KMS34 H929 KMS21 MOLP8 RPMI KMM1 KHM Del47 K28PE KMS20 KMM1 KMS28 MM1S KMS26 KMS12 JJN3 SKMM
B
[KMM1-38]
[KMS28BM-38]
[hIgG] [Elo-m] [Dara-m] [Isa]
[anti-hIgG /DAPI]
200 μm
Relative cell number (%)
hIgG Elo-m Dara-m Isa
FOXM1
E2F2
MCL1
GAPDH
C
DMSO Con-A
P < 0.05
Isa (μg/mL) 0 2.5 5
Con-A - + - + - +
D
KMM1-mock KMM1-FOX
KMS28-mock KMS28-FOX
Relative cell number (%)
Isatuximab (μg/mL)
[KMM1-38] [KMS28BM-38]
mock FOXM1
Control Isa
Relative ROS production(/10^5 cells)

Fig. 2

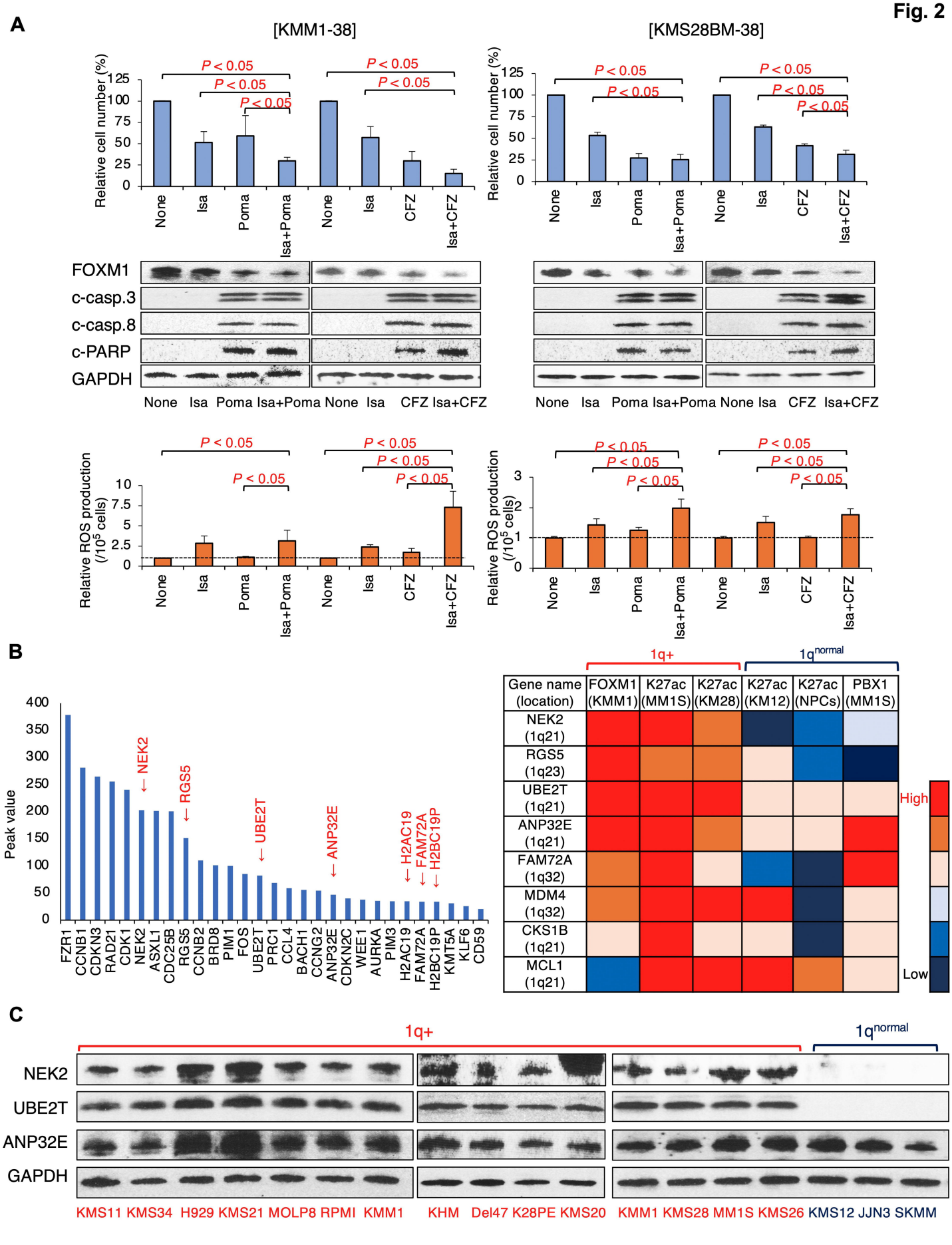
A
[KMM1-38]
[KMS28BM-38]
Relative cell number (%)
P < 0.05
None
Isa
Poma
Isa+Poma
CFZ
Isa+CFZ
FOXM1
c-casp.3
c-casp.8
c-PARP
GAPDH
Relative ROS production (/10^5 cells)
B
1q+
1q^normal
Gene name (location)
FOXM1 (KMM1)
K27ac (MM1S)
K27ac (KM28)
K27ac (KM12)
K27ac (NPCs)
PBX1 (MM1S)
NEK2 (1q21)
RGS5 (1q23)
UBE2T (1q21)
ANP32E (1q21)
FAM72A (1q32)
MDM4 (1q32)
CKS1B (1q21)
MCL1 (1q21)
High
Low
Peak value
FZR1 CCNB1 CDKN3 RAD21 CDK1 NEK2 ASXL1 CDC25B RGS5 CCNB2 BRD8 PIM1 FOS UBE2T PRC1 CCL4 BACH1 CCNG2 ANP32E CDKN2C WEE1 AURKA PIM3 H2AC19 FAM72A H2BC19P KMT5A KLF6 CD59
C
NEK2
UBE2T
ANP32E
GAPDH
KMS11 KMS34 H929 KMS21 MOLP8 RPMI KMM1 KHM Del47 K28PE KMS20 KMM1 KMS28 MM1S KMS26 KMS12 JJN3 SKMM

Fig. 3

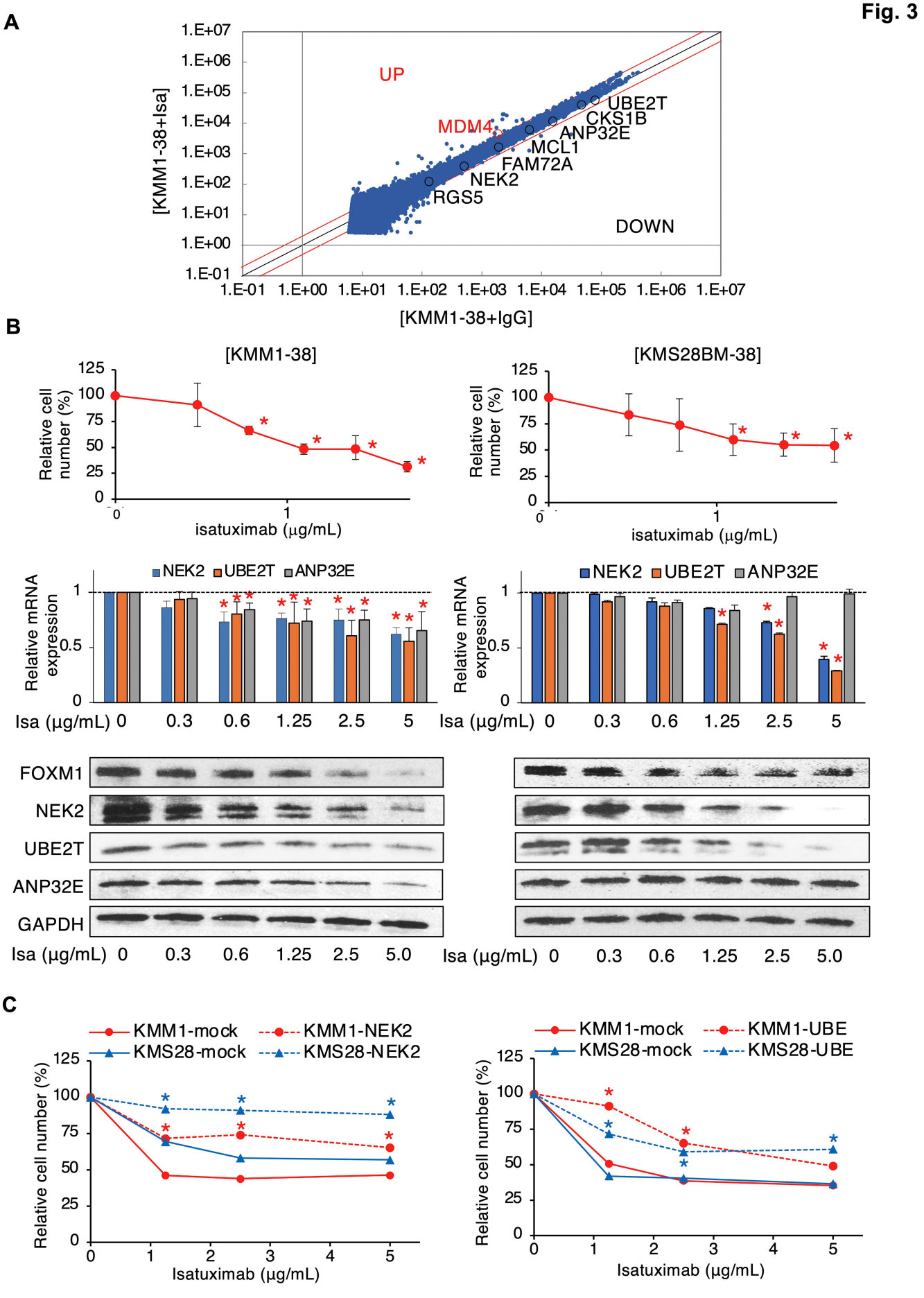
A
UP
DOWN
MDM4
UBE2T
CKS1B
ANP32E
MCL1
FAM72A
NEK2
RGS5
[KMM1-38+Isa]
[KMM1-38+IgG]
B
[KMM1-38]
[KMS28BM-38]
Relative cell number (%)
isatuximab (μg/mL)
NEK2
UBE2T
ANP32E
Relative mRNA expression
Isa (μg/mL) 0 0.3 0.6 1.25 2.5 5
FOXM1
NEK2
UBE2T
ANP32E
GAPDH
C
KMM1-mock
KMM1-NEK2
KMS28-mock
KMS28-NEK2
KMM1-UBE
KMS28-UBE
Relative cell number (%)
Isatuximab (μg/mL)

Fig. S1

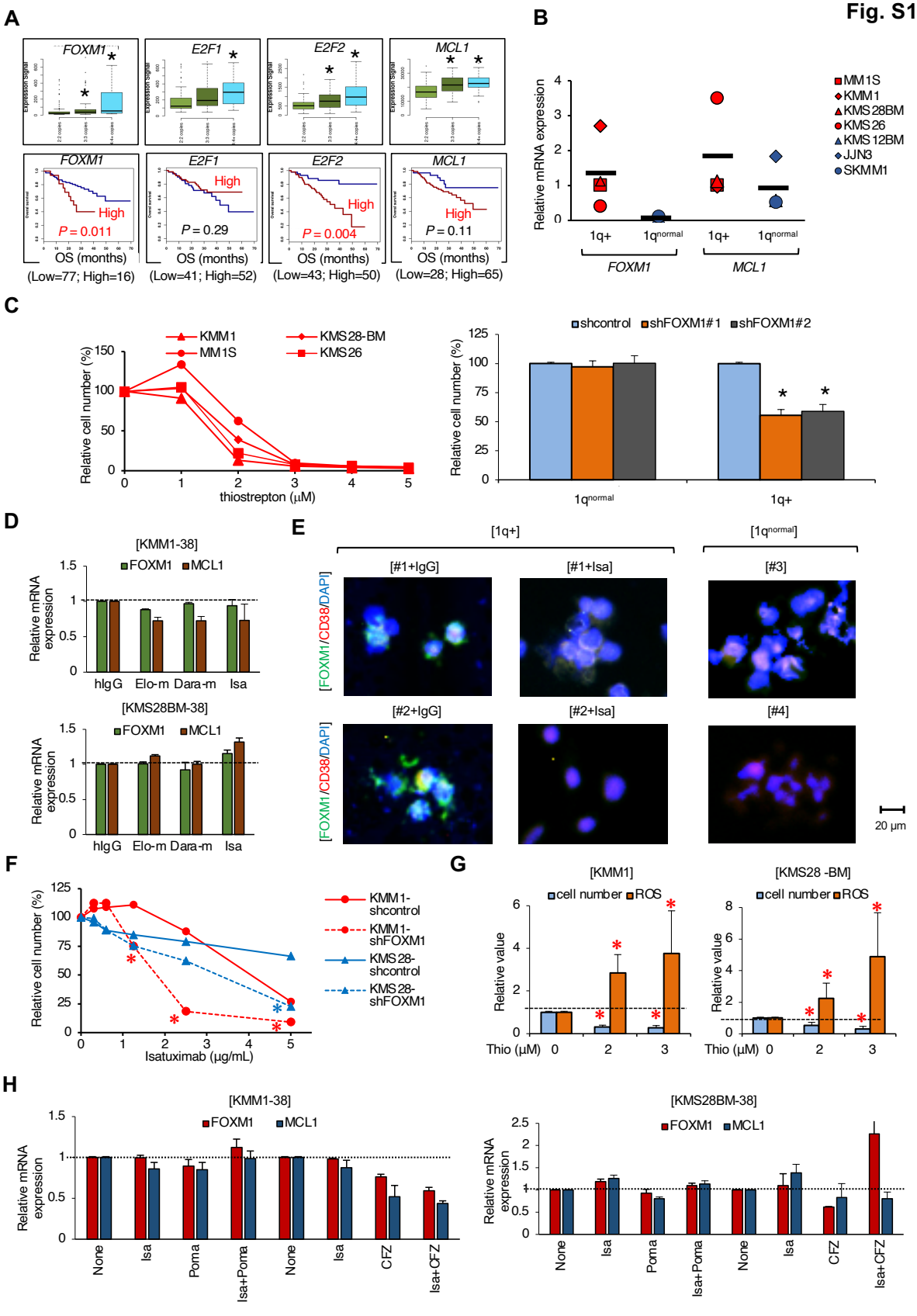
A
FOXM1
E2F1
E2F2
MCL1
High
P = 0.011
P = 0.29
P = 0.004
P = 0.11
OS (months)
(Low=77; High=16)
(Low=41; High=52)
(Low=43; High=50)
(Low=28; High=65)
B
Relative mRNA expression
MM1S
KMM1
KMS28BM
KMS26
KMS12BM
JJN3
SKMM1
1q+
1qnormal
FOXM1
MCL1
C
KMM1
MM1S
KMS28-BM
KMS26
Relative cell number (%)
thiostrepton (μM)
shcontrol
shFOXM1#1
shFOXM1#2
D
[KMM1-38]
[KMS28BM-38]
FOXM1
MCL1
Relative mRNA expression
hIgG
Elo-m
Dara-m
Isa
E
[1q+]
[1qnormal]
[#1+IgG]
[#1+Isa]
[#3]
[#2+IgG]
[#2+Isa]
[#4]
[FOXM1/CD38/DAPI]
20 μm
F
Relative cell number (%)
Isatuximab (μg/mL)
KMM1-shcontrol
KMM1-shFOXM1
KMS28-shcontrol
KMS28-shFOXM1
G
[KMM1]
[KMS28 -BM]
cell number
ROS
Relative value
Thio (μM)
H
[KMM1-38]
[KMS28BM-38]
FOXM1
MCL1
Relative mRNA expression
None
Isa
Poma
Isa+Poma
CFZ
Isa+CFZ

Supplementary Fig.S1. [A] Upper panels: The expression levels of *FOXM1*, *E2F1*, *E2F2*, and *MCL1* in MM cells with aberrant copy numbers of 1q. Lower panels: The prognostic significance of FOXM1, E2F2, E2F2, and MCL1 in the 1q+ MM patients. Kaplan-Meier curves showing the survival of MM patients with high (red) and low (blue) expression of each gene after total therapy 2 and 3 (TT2/3). *P* values were determined by the log-rank test. The GenomicScape tool (www.genomicscape.com) was used for the analysis. [B] Total RNAs were prepared from 1q+ MM cell lines (red) and $1q^{normal}$ MM cell lines (blue) and subjected to QPCR for *FOXM1* and *MCL1*. Data were quantified by the $2^{-\Delta\Delta Ct}$ method using *GAPDH* as the reference and are shown as fold changes against the value of MM.1S set at 1.0. We used TaqMan Fast Universal PCR Master Mix and Expression Assays (Hs01073586 for *FOXM1*, Hs06626047 for *MCL1*, and Hs01922876 for *GAPDH* (Thermo Fisher Scientific, MA, USA). [C] Left panel: KMM.1, KMS28BM, MM.1S, and KMS26 cells were treated with different concentrations of thiostreptone for 24 h. Cell proliferation was assessed by the MTT reduction assay and the data is shown relative to that of the corresponding untreated controls. Data are the means of multiple experiments (n > 3); S.D. was less than 10% and thus omitted. Right panel: The MM cell lines were transfected with shRNA targeting *FOXM1* (shFOXM1#1 and #2) or scrambled sequences (shcontrol) to 1q gain positive-KMM.1, KMS28-BM, or MM.1S cells (1q+), and 1q normal-KMS12BM, JJN3, or SK-MM1 cells ($1q^{normal}$). Cell proliferation was assessed by the MTT reduction assay and the data is shown relative to that of the corresponding sh-controls. Bars indicate the means of three MM cell lines. *P*-values were calculated by one-way ANOVA using a Student–Newman-Keuls multiple comparison test. The lentiviral short-hairpin RNA/short-interfering RNA (shRNA/siRNA) expression vector pLL3.7 was used for knockdown experiments. The siRNA sequences are as follows: #1; gaccactttccctacttta, #2; aagaagaaatcctggttaa. [D] KMM.1-38 and KMS28BM-38 cells were cultured in the absence or presence of 5 μg/mL human immunoglobulin (hIgG), elotuzumab-mimic (Elo-m), daratumumab-mimic (Dara-m), and isatuximab (Isa) for 24 h. Graphs show the expression levels of *FOXM1* and *MCL1* mRNAs relative to control IgG (values set at 1.0). The means ± S.D. (bars) of three independent experiments are shown. [E] CD138-positive cells were isolated from the bone marrow of MM patients and treated with 5 μg/ml hIgG or isatuximab (Isa) for 24 h. Cytospin specimens were prepared and stained with anti-FOXM1 antibody (green), and PE-conjugated anti-CD38 antibody (Red; BioLegend, CA, USA), followed by FITC-conjugated anti-rabbit IgG (Thermo Fisher Scientific). Nuclei were counterstained with DAPI (blue). Only merged images are shown. The copy number of chromosome 1q was detected by fluorescence in situ hybridization (FISH) using the CKS1B FISH probe; 1q gain was defined as having 3 copies of CKS1B, and 1q amp was

defined as having ≥4 copies of CKS1B. Patient #1 and #2 with ≥4 copies of chromosome 1q (1q+), and #3 and #4 with 2 copies of chromosome 1q ($1q^{normal}$). The FISH analyses were outsourced to SRL Inc. [F] KMM.1-38 and KMS28BM-38 cells were transduced with shFOXM1(#1) or shcontrol lentiviral vector and cultured with different concentrations of isatuximab (Isa) for 24 h. Cell proliferation was assessed by the MTT reduction assay and the data is shown relative to that of the corresponding untreated cells. Data are the means of multiple independent experiments (n > 3). S.D. was less than 10% and thus omitted; **P* < 0.05 by one-way ANOVA with Student-Newman-Keuls multiple comparison test. [G] KMM.1 and KMS28-BM cells were treated with different concentrations of the FOXM1 inhibitor thiostreptone (Thio) for 24 h. Cell proliferation was assessed by the MTT reduction assay and the data is shown relative to that of the corresponding untreated controls (blue bars). ROS levels were assessed using the ROS assay kit and the data is shown relative to that of the untreated controls (orange bars). Data are the means ± S.D. (bars) of multiple independent experiments (n = 3); **P* < 0.05 by one-way ANOVA with Student-Newman-Keuls multiple comparison test. [H] KMM.1-38 and KMS28BM-38 cells were treated with vehicle alone (None), 2.5 μg/ml isatuximab (Isa), 2 μM pomalidomide (Poma), 2 nM carfilzomib (CFZ), or their combinations (Isa+Poma or Isa+CFZ) for 24 h. The graphs show the expression levels of *FOXM1* and *MCL1* in the indicated groups. Data were quantified by the $2^{-\Delta\Delta Ct}$ method using *GAPDH* as the reference and are shown as fold changes against untreated control. The means ± S.D. (bars) of multiple independent experiments (n = 3) are shown.

Fig. S2

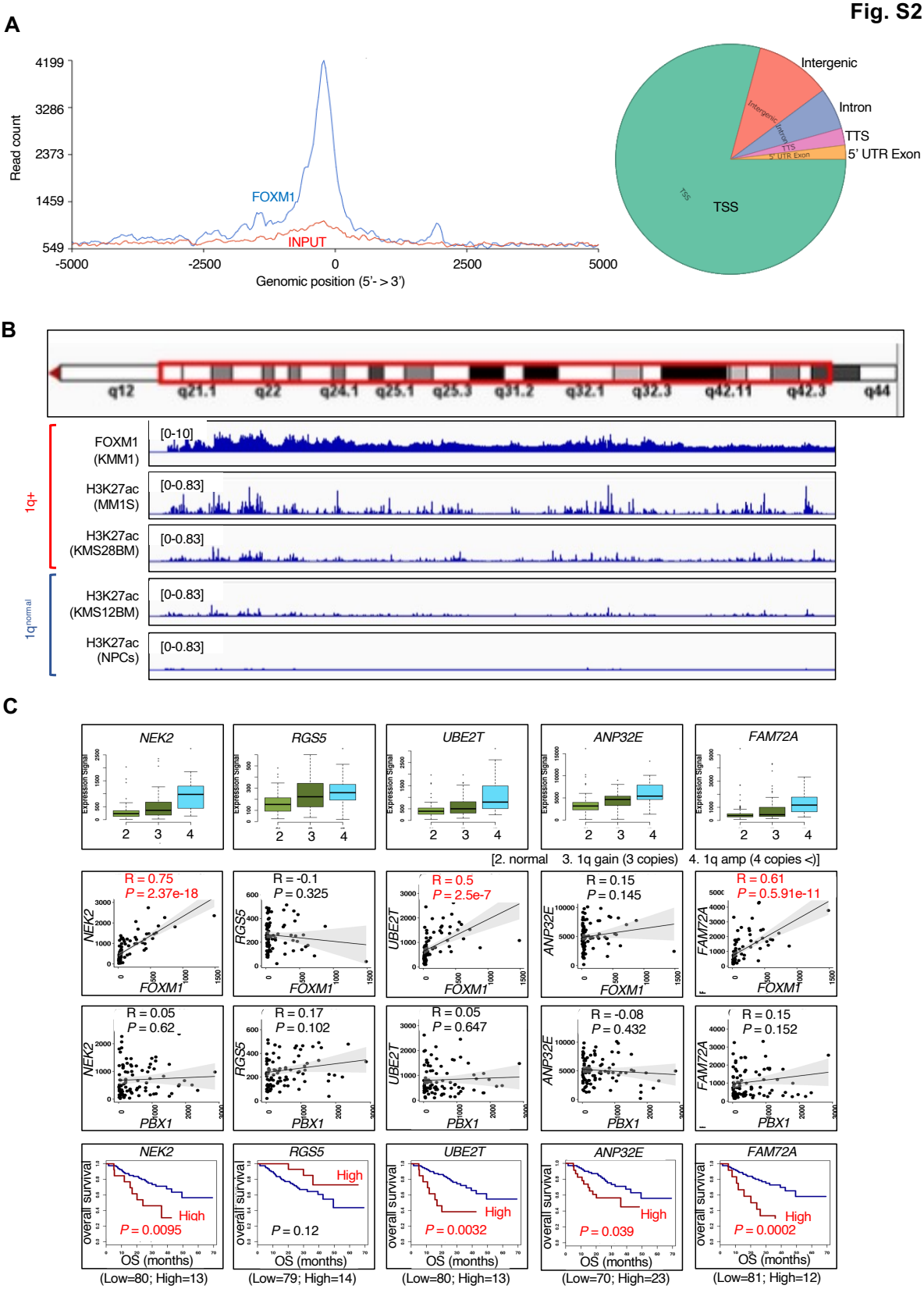
A
Read count
4199
3286
2373
1459
549
FOXM1
INPUT
-5000
-2500
0
2500
5000
Genomic position (5'- > 3')
Intergenic
Intron
TTS
5' UTR Exon
TSS
B
q12
q21.1
q22
q24.1
q25.1
q25.3
q31.2
q32.1
q32.3
q42.11
q42.3
q44
1q+
1q normal
FOXM1 (KMM1)
H3K27ac (MM1S)
H3K27ac (KMS28BM)
H3K27ac (KMS12BM)
H3K27ac (NPCs)
[0-10]
[0-0.83]
C
NEK2
RGS5
UBE2T
ANP32E
FAM72A
Expression Signal
2 3 4
[2. normal 3. 1q gain (3 copies) 4. 1q amp (4 copies <)]
R = 0.75
P = 2.37e-18
R = -0.1
P = 0.325
R = 0.5
P = 2.5e-7
R = 0.15
P = 0.145
R = 0.61
P = 0.5.91e-11
FOXM1
R = 0.05
P = 0.62
R = 0.17
P = 0.102
R = 0.05
P = 0.647
R = -0.08
P = 0.432
R = 0.15
P = 0.152
PBX1
overall survival
High
P = 0.0095
P = 0.12
P = 0.0032
P = 0.039
P = 0.0002
OS (months)
(Low=80; High=13)
(Low=79; High=14)
(Low=80; High=13)
(Low=70; High=23)
(Low=81; High=12)

Supplementary Fig.S2. [A] Left panel: Average plot of FOXM1 ChIP-seq reads over all transcription start sites (TSSs) ± 5,000 bp. Right panel: Pie chart showing gene section breakdown. [B] Visualization of the binding of FOXM1 and acetylated histone H3K27 (H3K27ac) on chromosome 1q region on the ChIP-Atlas platform. The ChIP-seq data of the following cell types was used: MM.1S (SRX20095564), KMS28BM (SRX7798959), KMS12BM (SRX7798957), and normal plasma cells isolated from healthy volunteers (NPCs) (SRX7798977). [C] Upper panel: The expression of possible target genes of FOXM1 (*NEK2*, RGS5, *UBE2T*, *AN32E*, and *FAM72A*) in MM cells with aberrant copy numbers of 1q. Middle panel: Correlation between the expression of FOXM1-target genes (y-axis) and the indicated genes (x-axis). Lower panel: The Kaplan-Meier curves indicate the survival of 1q+ MM patients with high (red) and low (blue) expression of FOXM1-target genes after TT2/3. *P* values were determined by a log-rank test. The GenomicScape tool (www.genomicscape.com) was used for the analyses.

Fig. S3

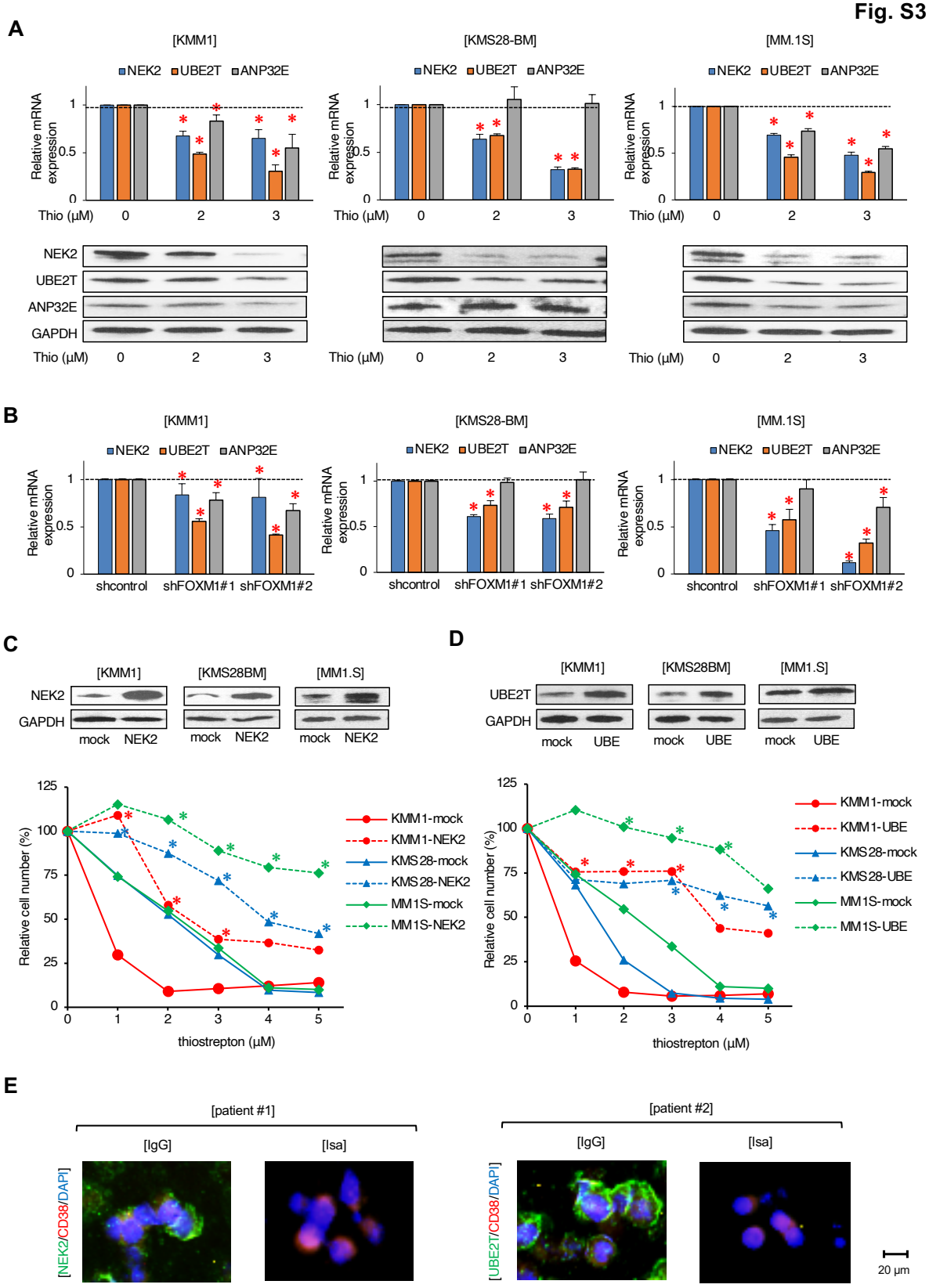
A
[KMM1]
[KMS28-BM]
[MM.1S]
NEK2 UBE2T ANP32E
Relative mRNA expression
Thio (μM) 0 2 3
NEK2
UBE2T
ANP32E
GAPDH
B
shcontrol shFOXM1#1 shFOXM1#2
C
[KMM1] [KMS28BM] [MM1.S]
mock NEK2
Relative cell number (%)
thiostrepton (μM)
KMM1-mock
KMM1-NEK2
KMS28-mock
KMS28-NEK2
MM1S-mock
MM1S-NEK2
D
UBE2T
mock UBE
KMM1-UBE
KMS28-UBE
MM1S-UBE
E
[patient #1]
[patient #2]
[IgG] [Isa]
[NEK2/CD38/DAPI]
[UBE2T/CD38/DAPI]
20 μm

Supplementary Fig.S3.

[A] KMM.1, KMS28BM, and MM.1S cells were treated with different concentrations of thiostreptone (Thio) for 24 h. Upper panel: QPCR results showing the expression levels of candidate FOXM1-target genes (*NEK2*, *UBE2T*, and *ANP32E*). Data were quantified by the $2^{-\Delta\Delta Ct}$ method using *GAPDH* as the reference and are shown as fold changes against untreated control. Data are the means ± S.D. (bars) of multiple independent experiments (n = 3). **P* < 0.05 by one-way ANOVA with a Student-Newman-Keuls multiple comparison test. Lower panel: Immunoblot showing the expression of NEK2, UBE2T, ANP32E, and GAPDH (loading control) in the indicated groups. [B] KMM.1, KMS28BM, and MM.1S cells were transduced with shFOXM1#1 and #2 or shcontrol. The expression levels of candidate FOXM1-target genes (*NEK2*, *UBE2T*, and *ANP32E*) are shown. Data were quantified by the $2^{-\Delta\Delta Ct}$ method using *GAPDH* as the reference and are shown as the fold changes against the values of shcontrol. Data are the means ± S.D. (bars) of multiple independent experiments (n = 3). **P* <0.05 by one-way ANOVA with Student-Newman-Keuls multiple comparison test. [C] KMM.1, KMS28BM, and MM.1S cells were transduced with either an empty lentiviral vector (mock) or NEK2-overexpressing vector (NEK2). Upper panel: Immunoblot showing expression of NEK2 and GAPDH (loading control) in the stable transformants. Lower panel: Each transformant was treated with different concentrations of thiostrepton at 24 h. Cell proliferation was assessed by the MTT reduction assay and the data is shown relative to that of the corresponding untreated controls. Data are the means of multiple experiments (n > 3); S.D. was less than 10% and thus omitted. **P* < 0.05 by one-way ANOVA with Student-Newman-Keuls multiple comparison test. [D] KMM.1, KMS28BM, and MM.1S cells were transduced with either an empty lentiviral vector (mock) or UBE2T-overexpressing vector (UBE). Upper panel: Immunoblot showing expression of UBE2T (UBE) and GAPDH (loading control) in the stable transformants. Lower panel: Each transformant was treated with different concentrations of thiostrepton at 24 h. Cell proliferation was assessed by the MTT reduction assay and the data is shown relative to that of the corresponding untreated controls. Data are the means of multiple experiments (n > 3); S.D. was less than 10% and thus omitted. **P* < 0.05 by one-way ANOVA with Student-Newman-Keuls multiple comparison test. [E] CD138-positive cells were isolated from the bone marrow of MM patients with 1q+ (patient #1 and #2) and treated with 5 μg/ml hIgG or isatuximab (Isa) for 24 h. Cytospin specimens were prepared and stained with anti-NEK2 antibody or anti-UBE2T antibody (green), and PE-conjugated anti-CD38 antibody (Red), followed by FITC-conjugated anti-rabbit IgG. Nuclei were counterstained with DAPI (blue). Only merged images are shown.